

# Spin moment formation and reduced orbital polarization in $\text{LaNiO}_3/\text{LaAlO}_3$ superlattice: LDA+ $U$ study

Myung Joon Han and Michel van Veenendaal

*Department of Physics, Northern Illinois University, De Kalb, Illinois 60115, USA and  
Advanced Photon Source, Argonne National Laboratory,  
9700 South Cass Avenue, Argonne, Illinois 60439, USA*

(Dated: January 26, 2012)

Density functional band calculations have been performed to study  $\text{LaNiO}_3/\text{LaAlO}_3$  superlattices. Motivated by recent experiments reporting the magnetic and metal-insulator phase transition as a function of  $\text{LaNiO}_3$  layer thickness, we examined the electronic structure, magnetic properties, and orbital occupation depending on the number of  $\text{LaNiO}_3$  layers. Calculations show that the magnetic phase is stabler than the nonmagnetic for finite and positive  $U$  values. The orbital polarization is significantly reduced by  $U$  even in the magnetic regions. The implications of the results are discussed in comparison to recent experimental and theoretical studies within the limitations of the LDA+ $U$  method.

PACS numbers: 73.20.-r, 75.70.-i, 71.15.Mb

## I. INTRODUCTION

Understanding transition metal oxides is of perpetual interest and importance in condensed matter physics and material science [1]. Recent advances in layer-by-layer growth techniques of heterostructures of transition metal compounds have created particular interest due to their great scientific and technological potential [2]. Exotic material phenomena that are clearly distinctive from the ‘normal’ phases include interface superconductivity [3], magnetism [4, 5], charge [6, 7] and orbital reconstruction [8].

One of the most intriguing classes of materials may be the nickelate superlattices [9–16]. A series of recent theoretical studies have created considerable interest, suggesting the heterostructuring-induced orbital polarization and the possible high- $T_c$  superconductivity in  $\text{LaNiO}_3$  (LAO)/ $\text{LaAlO}_3$  (LAO) superlattice [12, 17]. In this picture, the two degenerate Ni  $e_g$  orbital states are split by a combination of translational symmetry breaking and on-site Coulomb interaction, leading to a cuprate-like band structure. Although this kind of theoretical picture has been challenged by more recent dynamical mean-field theory (DMFT) calculations based on a charge transfer model including oxygen states explicitly [15], several experimental papers have found other interesting phenomena in this system. Boris and co-workers [10] reported a metal to insulator transition as a function of LNO layer thickness: Even though the bulk LNO is a paramagnetic (PM) metal, the heterostructure  $(\text{LNO})_m/(\text{LAO})_n$  becomes insulating and magnetic if  $m$  is small,  $m \leq 2$ , while it remains PM and metallic when  $m \geq 4$  [10]. The insulating behavior was also observed by Freeland *et al.* [13]. However the detailed magnetic and electronic structure changes, as well as the other important physical quantities such as orbital polarization have not yet been clearly understood as a function of layer thickness,  $m$ .

In this study, we performed a detailed first-principles

analysis for the electronic structure, magnetism, and orbital polarization of LNO/LAO superlattice using the LDA+ $U$  method [18–20]. Since previous calculations were performed at the LDA [14] or DMFT level [12, 15] and assumed the bulk-like PM phase, LDA+ $U$  calculation can provide meaningful information especially regarding the magnetism in this system. Total energy calculations showed that the LDA+ $U$  stabilizes ferromagnetic (FM) spin order along in-plane and out-of-plane direction. This result may indicate the existence of another ground state configuration in between  $m \sim 2$  and  $m \sim 4$  superlattices. The orbital polarization is significantly reduced by  $U$  which is in contrast to the simplified Hubbard-type model prediction [12], but consistent with the extended charge-transfer model DMFT calculation [15]. The calculated Ni- $d$  valence based on LDA+ $U$  supports the recently suggested picture for the metal/insulator phase diagram based on the  $d$ -valency [21], and demonstrates the importance of the double counting issue. These results are discussed in comparison to the recent theoretical and experimental studies.

## II. COMPUTATIONAL DETAILS

For the band-structure calculations, we employed Troullier-Martins type norm-conserving pseudopotential [22] with a partial core correction and linear combination of the localized pseudo-atomic orbitals (LCPAO) [23] as a basis set. In this pseudo-potential generation, the semi-core  $3p$  electrons for transition metal atoms were included as valence electrons in order to take into account the contribution of the semi-core states to the electronic structure. We adopted the local density approximation (LDA) for exchange-correlation energy functional as parametrized by Perdew and Zunger [24], and used energy cutoff of 400 Ry and k-grid of  $12 \times 12 \times 6$  per unit superlattice volume. The LDA+ $U$  functional is adapted from the formalism of Ref. 26 and Ref. 25 [27]. The

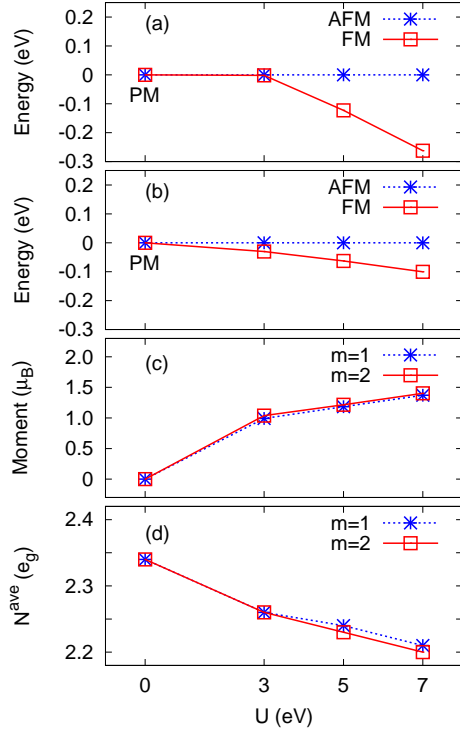


FIG. 1: (Color online) (a) Calculated total energy of (LNO)<sub>1</sub>/(LAO)<sub>1</sub> with the in-plane spin ordering of FM and AFM as a function of  $U$ . (b) Calculated total energy of (LNO)<sub>2</sub>/(LAO)<sub>1</sub> with the out-of-plane spin ordering of FM and AFM as a function of  $U$  where the in-plane spins are set to be FM. (c) Calculated Ni magnetic moment for (LNO)<sub>1</sub>/(LAO)<sub>1</sub> and (LNO)<sub>2</sub>/(LAO)<sub>1</sub> as a function of  $U$  (FM order considered). (d) Average number of Ni- $e_g$  electrons in (LNO)<sub>1</sub>/(LAO)<sub>1</sub> and (LNO)<sub>2</sub>/(LAO)<sub>1</sub> as a function of  $U$ .

geometry relaxation has been performed with the force criterion of  $10^{-3}$  Hartree/Bohr. During the relaxation process, the in-plane lattice constant is fixed considering the substrate effect in the experimental situation. The orbital polarization  $P$ , defined as

$$P = \frac{n_{x^2-y^2} - n_{3z^2-r^2}}{n_{x^2-y^2} + n_{3z^2-r^2}}, \quad (1)$$

can be calculated by integrating the projected density-of-states (DOS) up to Fermi level. All the calculations were performed using the density functional theory code OpenMX [28].

### III. RESULT AND DISCUSSION

One natural and evidently important question raised from experimental studies on the magnetic moment formation in this heterostructure [10] is about the ground state spin structure and its moment size. Fig. 1 summarizes our results. Fig. 1(a) shows the calculated total energy of (LNO)<sub>1</sub>/(LAO)<sub>1</sub> superlattice as a function of  $U$ . While at  $U=0$  eV both FM and antiferromagnetic



FIG. 2: (Color online) The suggested schematic phase diagram (based on the previous experiment and our calculation) of the possible ground state configuration of (LNO)<sub>m</sub>/(LAO)<sub>n</sub> as a function of  $m$  (see the text).

(AFM) spins eventually converge to a PM solution, the magnetic ground states are stabilized at the finite  $U$ . As clearly seen in Fig. 1(a), FM spin ordering is energetically favored within the LNO plane. The energy difference between FM and AFM state is 3, 246, and 525 meV per (LNO)<sub>1</sub>/(LAO)<sub>1</sub> for  $U=3, 5$ , and  $7$  eV, respectively. FM spin order is also favored along the out-of-plane direction as shown in Fig. 1(b) in which we present total energies of (LNO)<sub>2</sub>/(LAO)<sub>1</sub>; the out-of-plane spin orderings are set to be FM or AFM while the in-plane order is FM. The calculated FM-AFM energy difference is 60, 126, and 201 meV per (LNO)<sub>2</sub>/(LAO)<sub>1</sub> for  $U=3, 5, 7$  eV, respectively. The energy differences between FM and AFM spin structure becomes larger as  $U$  increases in both cases of in-plane and out-of-plane ordering. That is, the on-site correlations stabilize FM spin ordering, and as  $U$  decreases, the two magnetic solutions becomes more close in their energies, and eventually converges to the PM phase at  $U=0$ . The magnetic moment is also dependent on  $U$ . Fig. 1(c) shows the calculated magnetic moment for FM case as a function of  $U$ . The moment increases as  $U$  increases as in the other typical correlated transition metal oxide materials [18, 20, 25]. It is noted that, as soon as  $U$  is turned on, the Ni moment becomes  $\sim 1 \mu_B$  ( $U=3$  eV), and further increases to be  $1.2$  and  $1.4 \mu_B$  at  $U=5$  and  $7$  eV, respectively.

Our calculation results may seem to suggest that the magnetic moment formed in the thin-LNO superlattice [10] is ordered ferromagnetically. Since the spin polarized oxide heterostructure could be useful for the device applications, there has been active research for finding the structure that produces FM spin order [29–31]. Therefore our result of a FM ground state in LNO/LAO may have a positive implication for such an application. However it should be noted that the muon spin rotation ( $\mu$ SR) experiment by Boris *et al.* [10] is not well interpreted in the long range FM ordering picture even though the  $\mu$ SR

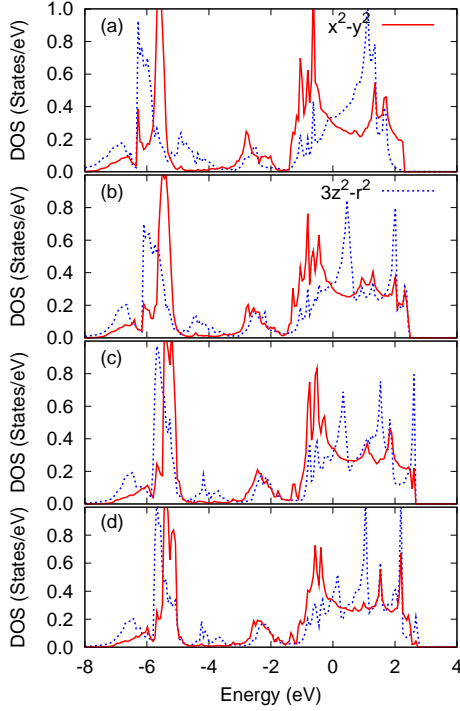


FIG. 3: (Color online) Ni- $e_g$  DOS of  $(\text{LNO})_m/(\text{LAO})_1$  superlattice geometry with PM spin ( $U=0$ ): (a)  $m=1$ , (b)  $m=2$ , (c)  $m=3$ , and (d)  $m=4$ . Solid (red) and dotted (blue) lines correspond to  $d_{x^2-y^2}$  and  $d_{3z^2-r^2}$  states, respectively, and Fermi level is set to be 0.

is basically a local probe and that the origin of metal-insulator phase transition in the nickelate series are not clearly understood yet. Especially regarding the charge disproportion or ordering in nickelates, the conventional LDA+ $U$  has a clear limitation to describe such phenomena [32, 33]. Moreover Fig. 1(a) and (b) indicate the possibility of AFM ground state in the negative  $U$  region which is more or less related to the reported charge disorders in the nickelate systems [32, 33]. Therefore one needs to be careful in the interpretation of our LDA+ $U$  results on the FM spin ground state as an indication of long range ordered ground state as one may see in the actinide systems for example [34, 35].

Our results have another interesting implication regarding the phase diagram. Since the thin-LNO superlattice,  $(\text{LNO})_{m \leq 2}/(\text{LAO})_n$ , can have either FM insulating (FM-I) ground state as predicted by LDA+ $U$  calculations, or, AFM insulating (AFM-I) one which is more consistent with the  $\mu\text{SR}$  experiment, the system would have FM metallic (FM-M) or AFM metallic (AFM-M) region in between the thin-LNO limit ( $m \leq 2$ ), and the bulk-like thick-LNO limit ( $m \geq 4$ ; PM and metallic, PM-M) [10]. One may also expect the PM insulating (PM-I) phase stabilized in the same region of  $m$ ; the intermediate regime,  $2 \leq m \leq 4$  (see, Fig. 2). As LDA+ $U$  method is unable to describe correlated PM solutions properly [36, 37], the further pursue along this line is beyond the scope of our study. For that purpose, one may resort the

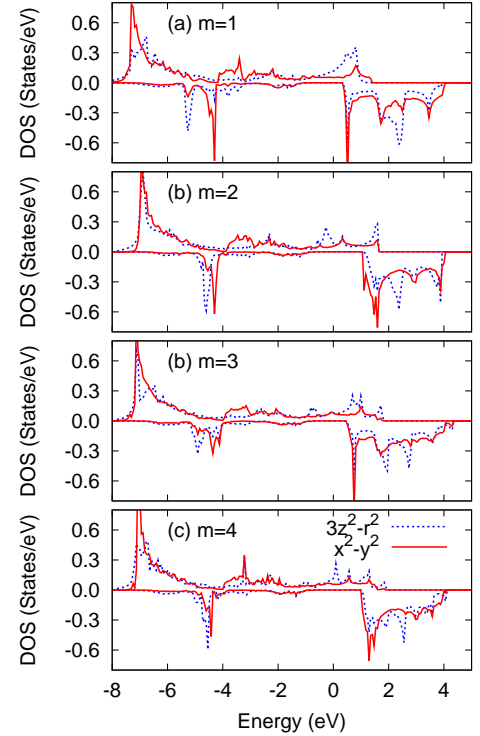


FIG. 4: (Color online) Ni- $e_g$  DOS of  $(\text{LNO})_m/(\text{LAO})_1$  superlattice geometry with FM spin ( $U=5$  eV): (a)  $m=1$ , (b)  $m=2$ , (c)  $m=3$ , and (d)  $m=4$ . Up/down panels represent the up/down spin states, respectively. Solid (red) and dotted (blue) lines correspond to  $d_{x^2-y^2}$  and  $d_{3z^2-r^2}$  states, respectively, and the Fermi level is set to be 0.

dynamical mean field theory (DMFT) calculations with charge self-consistency [36, 37], and compare the total energy for PM, FM and AFM configurations as we did in this study within LDA+ $U$  scheme.

To understand metal-insulator phase transition as a function of LNO thickness [10], we examined Ni  $e_g$  DOS depending on the thickness,  $m$ . The  $d$ -band width change as a function of  $m$  may be an useful information as  $U/W$  plays an important role in the metal-insulator phase transition of rare-earth nickelate [38]. Fig. 3 shows DOS of the PM case with  $U=0$ . Even if the bulk LNO locates at the vicinity of metal-insulator phase boundary and exhibits the correlated electron behaviors, the electronic structure of PM LNO has been reasonably well described within LDA (or GGA) as shown in the previous studies [14, 38, 39]. Fig. 3(a)-(d) presents the evolution of  $e_g$  DOS as a function of  $m$ . It is noted that the  $d_{3z^2-r^2}$  band width notably changes, whereas the  $d_{x^2-y^2}$  width remains almost same across  $m=2-4$ . The  $m=2$  case (Fig. 3(b)), which was reported to be magnetic and insulating [10], the right edge of the  $d_{3z^2-r^2}$  state is fairly similar to that of  $d_{x^2-y^2}$  whereas the left-edge is reduced. It is not certain however that such a relatively small difference in terms of the effective band width is responsible for the metal-insulator phase transition between  $m=2$  and 4 as reported in experiment [10].

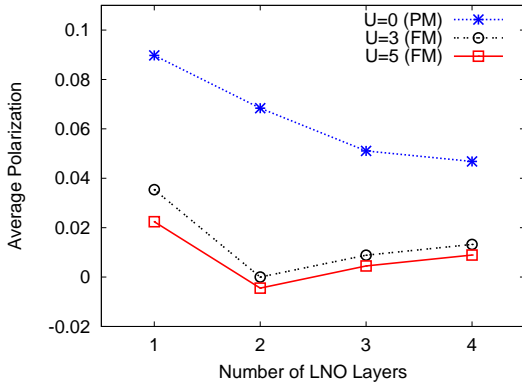


FIG. 5: (Color online) The averaged orbital polarization as a function of LNO layer thickness. Dotted (blue, double cross), double-dotted (black, circle), and solid (red, square) lines represent  $U=0$  (PM),  $U=3$  (FM), and  $U=5$  (FM), respectively.

A complementary picture can be provided by LDA+ $U$  calculations for the magnetic phase. Fig. 4(a)-(d) shows the evolution of  $e_g$  DOS as a function of  $m$  for the FM  $(\text{LNO})_1/(\text{LAO})_1$ . Once again the notable change is found in  $d_{3z^2-r^2}$  band; for  $m=1$ , the up-spin  $d_{3z^2-r^2}$  state (upper panel) forms a fairly localized DOS around Fermi level. This state becomes more and more delocalized as  $m$  increases as seen in Fig. 4(b)-(d). Once again, however, the amount of the effective band width change depending on  $m$  does not seem to be enough to make metal-insulator phase transition across  $m=2-4$ . Other origins than the simple  $U/W$  change may be more relevant to the transition [21, 32].

An interesting point observed in Fig. 4 is that even in LDA+ $U$  calculation, the systems do not become a perfect insulator, but have finite number of states around Fermi level [40]. It may partly be attributed to the strong covalency between Ni- $d$  and O- $p$  states. As O- $p$  is much less affected by  $U$ , the small amount of DOS is not removed perfectly. Another important factor is the double-counting energy correction for which several functional forms have been suggested [18–20, 25, 26], but there is no well defined solution still yet [21]: As the double-counting energy is typically represented by  $\frac{1}{2}UN_d(N_d - 1)$ , the LDA+ $U$  charge self-consistency adjusts  $N_d$  (or, the effective  $d$ -level energy and therefore the charge transfer energy,  $\epsilon_p - \epsilon_d$ ), depending on  $U$ . According to the recent DMFT study, which tunes the double-counting term as a parameter, the system eventually becomes insulating at large  $U$  [15, 41]. Therefore the small states around the Fermi level obtained by LDA+ $U$  can be attributed to the double-counting error that is hardly handled within the current formalism of LDA+ $U$ .

An interesting recent finding on (3-dimensional) nickelates is that the metal-insulator transition occurs at the very narrow region of  $N_d$  and the same holds for the cuprates [21]. From the single-site DMFT calculations with a double-counting energy as another tuning parameter, Wang *et al.* [21] showed that there is a well defined

$N_c$ , that is, the critical value of  $d$ -valency of transition metal; the system is metallic if  $N_d \geq N_c$  and insulating if  $N_d \leq N_c$ . For nickelates,  $N_c^{e_g} \approx 1.3$ . That is, for the parameters (implicitly including double-counting correction), which result in  $N_d \geq N_c$ , the system remains metallic even for the very large  $U$ . This conclusion suggests  $N_d$  as the critical variable for understanding charge-transfer systems [21]. Now it might be instructive to analyze our LDA+ $U$  results within this new picture of Ref. 21. Even if LDA+ $U$  is a lower level approximation compared to DMFT, a big merit of LDA+ $U$  is that it can be performed with the whole charge self-consistency and take magnetism into account while the previous DMFT calculations have dealt with the PM phase [12, 15]. Fig. 1(d) presents  $N_d$  for PM ( $U=0$ ) and FM ( $U=3, 5, 7$ ) calculations of  $(\text{LNO})_{m=1}/(\text{LAO})_1$  and  $(\text{LNO})_{m=2}/(\text{LAO})_1$ . While  $N_d$  decreases as  $U$  increases, the difference is not significant;  $\Delta N_d \approx 0.15$ . Therefore the current implementation of LDA+ $U$  and the charge self-consistency roughly follow the constant  $N_d$  line. Now we note that the value of  $N_d^{e_g} \geq 2.2$  is far from the  $N_c \approx 1.3$  predicted by DMFT. Therefore it is consistent with the metallic ground state and supports the conclusion of Ref. 21.

Relative orbital occupation in the two  $e_g$  orbitals is a central quantity in understanding LNO/LAO systems [9, 12, 14, 15]. The orbital polarization can be non-zero due to the translation symmetry breaking induced by heterostructuring while the bulk polarization is 0. According to the previous calculations, highly polarized  $P$  can possibly drives the system to be high- $T_c$  superconductor [12, 17]. On the other hand, a more recent DMFT calculation based on the realistic model hamiltonian including oxygen orbitals predicted that the polarization is actually reduced by the on-site correlation [15]. Since both of the previous DMFT calculations assumed PM phase and did not consider the full charge self-consistency, LDA+ $U$  calculation can give a complementary information for the magnetic solution in spite of its limitation in describing correlation effect compared to DMFT. The result is presented in Fig. 5. It is noted that the inclusion of  $U$  reduces the polarization significantly. There is a large separation between  $U=0$  and  $U=3$  results, while the differences between  $U=3$  and 5 results are small. Importantly the calculated polarizations for finite  $U$  are order-of-magnitude same compared with the recent DMFT results [15]. Therefore it supports the conclusion of the recent DMFT calculation [15]. The small polarization at the finite  $U$  can also be seen in DOS presented in Fig. 4 where no big difference can be found between the two  $e_g$  orbital occupations. We note that the reduced orbital polarization by  $U$  can be compatible with the ferromagnetic spin order. For cuprates, for example, the fully polarized  $x^2 - y^2$  orbital is directly related to the in-plane AFM spin order. In the nickelates, we have one more orbital degree of freedom available and the spin can align ferromagnetically. And actually it is found that the enhanced ferromagnetic trend by increas-

ing  $U$  corresponds to the reduced orbital polarization as shown in Fig. 5.

#### IV. SUMMARY

Using the band structure calculations based on LDA+ $U$ , we examined the magnetic moment, electronic structure,  $d$ -valence, and orbital polarization as a function of  $U$  and  $m$  (LNO thickness). The calculated results clearly showed the formation of magnetic moment at the finite  $U$  region being consistent with a recent  $\mu$ SR, but the long range ordering pattern is not so clear considering the experiment. While  $d_{3z^2-r^2}$  band width is reduced as  $m$  approaches to 1, it may not be enough to

be responsible for the metal-insulator transition. The calculated orbital polarization is significantly reduced by  $U$ , strongly supporting the conclusion of a recent DMFT calculations and indicating the absence of high temperature superconductivity in this system.

#### V. ACKNOWLEDGMENTS

This work was supported by the U.S. Department of Energy (DOE), DE-FG02-03ER46097, and NIUS Institute for Nanoscience, Engineering, and Technology. Work at Argonne National Laboratory was supported by the U.S. DOE, Office of Science, Office of Basic Energy Sciences, under Contract No. DE-AC02-06CH11357.

- 
- [1] M. Imada, A. Fujimori, and Y. Tokura, Rev. Mod. Phys. **70**, 1039 (1998).
  - [2] For a review, see, J. Mannhart, D. H. A. Blank, H. Y. Hwang, A. J. Millis, and J. M. Triscone, Bulletin of the Materials Research Society **33**, 1027 (2008).
  - [3] N. Reyren, S. Thiel, A. D. Caviglia, L. F. Kourkoutis, G. Hammerl, C. Richter, C. W. Schneider, T. Kopp, A.-S. Rüetschi, D. Jaccard, M. Gabay, D. A. Muller, J.-M. Triscone, J. Mannhart, Science **317**, 1196 (2007).
  - [4] L. Li, C. Richter, J. Mannhart, and R. C. Ashoori, Nature Phys. **7**, 762 (2011).
  - [5] J. A. Bert, B. Kalisky, C. Bell, M. Kim, Y. Hikita, H. Y. Hwang, and K. A. Moler, Nature Phys. **7**, 767 (2011).
  - [6] A. Ohtomo, D. A. Muller, J. L. Grazul, and H. Y. Hwang, Nature **419**, 378 (2002).
  - [7] S. Okamoto and A. J. Millis, Nature **428**, 630 (2004).
  - [8] J. Chakhalian, J. W. Freeland, H.-U. Habermeier, G. Cristiani, G. Khaliullin, M. van Veenendaal, and B. Keimer, Science **318**, 1114 (2007).
  - [9] E. Benckiser, M. W. Haverkort, S. Brck, E. Goering, S. Macke, A. Fra, X. Yang, O. K. Andersen, G. Cristiani, H.-U. Habermeier, A. V. Boris, I. Zegkinoglou, P. Wochner, H.-J. Kim, V. Hinkov and B. Keimer, Nature Mater. **10**, 493 (2011).
  - [10] A. V. Boris, Y. Matiks, E. Benckiser, A. Frano, P. Popovich, V. Hinkov, P. Wochner, M. Castro-Colin, E. Detemple, V. K. Malik, C. Bernhard, T. Prokscha, A. Suter, Z. Salman, E. Morenzoni, G. Cristiani, H.-U. Habermeier, and B. Keimer, Science **332**, 937 (2011).
  - [11] J. Liu, S. Okamoto, M. van Veenendaal, M. Kareev, B. Gray, P. Ryan, J. W. Freeland, and J. Chakhalian, Phys. Rev. B **83** 161102, (2011).
  - [12] P. Hansmann, X. Yang, A. Toschi, G. Khaliullin, O. K. Andersen, and K. Held, Phys. Rev. Lett. **103**, 016401 (2009).
  - [13] J. W. Freeland, J. Liu, M. Kareev, B. Gray, J.W. Kim, P. Ryan, R. Pentcheva, and J. Chakhalian, arXiv:1008.1518 (2010).
  - [14] M. J. Han, C. A. Marianetti, and A. J. Millis, Phys. Rev. B **82** 134408, (2010).
  - [15] M. J. Han, X. Wang, C. A. Marianetti, and A. J. Millis, Phys. Rev. Lett. **107** 206804, (2011).
  - [16] M. K. Stewart, J. Liu, M. Kareev, J. Chakhalian, and D. N. Basov, Phys. Rev. Lett. **107** 176401, (2011).
  - [17] J. Chaloupka and G. Khaliullin, Phys. Rev. Lett. **100**, 016404 (2008).
  - [18] V. I. Anisimov, J. Zaanen, and O. K. Andersen, Phys. Rev. B **44**, 943 (1991).
  - [19] A. I. Liechtenstein, V. I. Anisimov, and J. Zaanen, Phys. Rev. B **52**, R5467 (1995).
  - [20] V. I. Anisimov, F. Aryasetiawan, and A. I. Liechtenstein, J. Phys.:Condens. Matter **9**, 767 (1997);
  - [21] X. Wang, M. J. Han, L. de' Medici, C. A. Marianetti, and A. J. Millis, arXiv:1110.2782 (2011).
  - [22] N. Troullier and J. L. Martins, Phys. Rev. B **43**, 1993 (1991).
  - [23] T. Ozaki, Phys. Rev. B **67**, 155108, (2003); T. Ozaki and H. Kino, Phys. Rev. B **69**, 195113, (2004); T. Ozaki and H. Kino, J. Chem. Phys. **121**, 10879, (2004).
  - [24] D. M. Ceperley and B. J. Alder, Phys. Rev. Lett. **45**, 566(1980); J. P. Perdew and A. Zunger, Phys. Rev. B **23**, 5048 (1981).
  - [25] M. J. Han, T. Ozaki, and J. Yu, Phys. Rev. B **73**, 045110 (2006).
  - [26] S. L. Dudarev, G. A. Botton, S. Y. Savrasov, C. J. Humphreys, and A. P. Sutton, Phys. Rev. B **57**, 1505 (1998).
  - [27] In this formalism, the effective on-site Coulomb interaction is represented by  $U$  (on-site Coulomb repulsion) –  $J$  (Hund's interaction).
  - [28] <http://openmx-square.org>
  - [29] U. Lüders, W. C. Sheets, A. David, W. Prellier, and R. Frésard, Phys. Rev. B **80**, 241102 (2009).
  - [30] J. D. Burton and E. Y. Tsymbal, Phys. Rev. Lett. **107** 166601, (2011).
  - [31] B. R. K. Nanda and S. Satpathy, Phys. Rev. Lett. **101** 127201, (2008).
  - [32] I. I. Mazin, D. I. Khomskii, R. Lengsdorf, J. A. Alonso, W. G. Marshall, R. M. Ibberson, A. Podlesnyak, M. J. Martinez-Lope, and M. M. Abd-Elmeguid, Phys. Rev. Lett. **98**, 176406 (2007).
  - [33] M. Medarde, C. Dallera, M. Grioni, B. Delley, F. Vernay, J. Mesot, M. Sikora, J. A. Alonso, and M. J. Martinez-Lope, Phys. Rev. B **80**, 245105 (2009).
  - [34] K. T. Moore and G. van der Laan, Rev. Mod. Phys. **81**, 235 (2009).

- [35] M. J. Han, X. Wan, and S. Y. Savrasov, Phys. Rev. B **78**, 060401 (2008).
- [36] A. Georges, G. Kotliar, W. Krauth, and M. J. Rozenberg, Rev. Mod. Phys. **68**, 13 (1996).
- [37] G. Kotliar, S. Y. Savrasov, K. Haule, V. S. Oudovenko, O. Parcollet, and C. A. Marianetti, Rev. Mod. Phys. **78**, 865 (2006).
- [38] S. R. Barman, A. Chainani, and D. D. Sarma, Phys. Rev. B **49**, 8475 (1994).
- [39] M. J. Han and Michel van Veenendaal, Phys. Rev. B. **84** 125137, (2011).
- [40] We found that this feature is retained up to  $U = 9$  eV, and for the larger  $U$ , the charge convergency is not well stabilized.
- [41] It should be noted that the effective  $U$  values, used in the self-consistent LDA+ $U$  calculation and in the effective model DMFT one, can not be directly compared.